Supporting Information

Experimental Proofs for Emission Annihilation through the Bond Elongation at the Carbon-Carbon Bond in *o*-Carborane with Fused Biphenyl-Substituted Compounds

Junki Ochi, Kazuo Tanaka* and Yoshiki Chujo

Department of Polymer Chemistry, Graduate School of Engineering, Kyoto University Katsura, Nishikyo-ku, Kyoto 615-8510, Japan

E-mail: tanaka@poly.synchem.kyoto-u.ac.jp

General.

^{1}H, ^{13}C, and ^{11}B NMR spectra were recorded on a JEOL JNM-AL400 instrument at 400, 100, and 128 MHz, respectively. Samples were analyzed in $CDCl_3$ and CD_2Cl_2. The ^{1}H and ^{13}C chemical shift values were expressed relative to Me_4Si as an internal standard in $CDCl_3$. The ^{11}B chemical shift values were expressed relative to $BF_3{\cdot}Et_2O$ as an external standard. Analytical thin-layer chromatography (TLC) was performed with silica gel 60 Merck F254 plates. Column chromatography was performed with Wakogel® C-300 silica gel. High-resolution mass (HRMS) spectrometry was performed at the Technical Support Office (Department of Synthetic Chemistry and Biological Chemistry, Graduate School of Engineering, Kyoto University), and the HRMS spectra were obtained on a Thermo Fisher Scientific EXACTIVE spectrometer for atmospheric pressure chemical ionization (APCI). UV–vis absorption spectra were obtained on a SHIMADZU UV3600 spectrophotometer. Photoluminescence (PL) spectra were measured with a HORIBA JOBIN YVON Fluorolog-3 spectrofluorometer. Fluorescence quantum yield (QY) was recorded on a HAMAMATSU Quantaurus-QY Plus C13534-01 model. The PL lifetime measurement was performed on a Horiba FluoroCube spectrofluorometer system; excitation was carried out using a UV diode laser (NanoLED 292 nm). X-ray crystallographic analysis was carried out by Rigaku R-AXIS RAPID-F graphite-monochromated Mo-Kα radiation diffractometer with imaging plate. A symmetry-related absorption correction was carried out by using the program ABSCOR[1]. The structures were solved with SHELXT 2014[2] and refined on F^2 with SHELXL[3] on Yadokari-XG.[4] All hydrogen atoms were placed at calculated positions and refined using a riding model. The program Mercury 4.2.0[5] was used to generate the X-ray structural diagram.

Materials.

Commercially available compounds used without purification:

Decaborane (Toronto Research Chemicals, Inc.)

N,*N*-Dimethylaniline (FUJIFILM Wako Pure Chemical Industries, Ltd.)

n-Butyllithium (1.6 M in THF) (Kanto Chemical Co, Inc.)

t-Butyldimethylsilyl trifluoromethanesulfonate (FUJIFILM Wako Pure Chemical Industries, Ltd.)

Palladium(II) acetate (FUJIFILM Wako Pure Chemical Industries, Ltd.)

Tri-*tert*-butylphosphonium tetrafluoroborate (Tokyo Chemical Industry Co, Ltd.)

Cesium carbonate (FUJIFILM Wako Pure Chemical Industries, Ltd.)

Cesium fluoride (FUJIFILM Wako Pure Chemical Industries, Ltd.)

Commercially available solvents:

MeOH (Wako Pure Chemical Industries, Ltd.), $CHCl_3$ (Wako Pure Chemical Industries, Ltd.), *n*-hexane (Wako Pure Chemical Industries, Ltd.), AcOEt (Wako Pure Chemical Industries, Ltd.), toluene (deoxidized grade, Wako Pure Chemical Industries, Ltd.) and MeCN (deoxidized grade, Wako Pure Chemical Industries, Ltd.) and acetone (deoxidized grade, Wako Pure Chemical Industries, Ltd.) were used without further purification. Et_2O (deoxidized grade, Wako Pure Chemical Industries, Ltd.) were purified by passage through solvent purification columns under N_2 pressure.

Compounds prepared as described in the literatures:

2-Bromo-2'-ethynyl-1,1'-biphenyl[6]

Synthesis of 1. The mixture of 2-bromo-2'-ethynyl-1,1'-biphenyl (1.06 g, 4.12 mmol), decaborane (0.581 g, 4.76 mmol), and *N*,*N*-dimethylaniline (0.894 g, 0.93 ml, 7.38 mmol) were dissolved in dry toluene (41 ml) at room temperature under N_2 atmosphere. The mixture was refluxed for 7 h. After cooling to room temperature, the mixture was filtrated and evaporated. The residue was recrystalized from MeOH to afford **1** as a white solid (1.01 g, 2.69 mmol, 66%). ^{1}H NMR (400 MHz, CD_2Cl_2): δ (ppm) 7.78–7.72 (2H, Ar-*H*), 7.44–7.29 (5H, Ar-*H*), 7.01 (1H, m, Ar-*H*), 3.28 (1H, s, carborane_C-*H*), 3.44–1.09 (10H, br, B-*H*). ^{13}C NMR (100 MHz, CD_2Cl_2): δ (ppm) 140.9, 138.6, 133.8, 133.0, 132.8, 131.8, 131.2, 131.0, 129.2, 128.9, 127.7, 124.2, 77.5, 58.5. ^{11}B NMR (128 MHz, $CDCl_3$): δ (ppm) –3.0, –4.2, –8.6, –9.9, –12.0, –13.2, –14.4. HRMS (*n*-APCI): Calcd. for $C_{14}H_{19}B_{10}Br$ $[M]^-$ m/z 376.1658, found m/z 376.1652.

Synthesis of 2. *n*BuLi (0.65 mL, 1.6 M in hexane, 1.04 mmol) was added dropwise to the mixture of **1** (0.376 g, 1.00 mmol) and anhydrous diethyl ether (10 ml) at –78 °C. After addition, the mixture was stirred for 2 h at the same temperature, then TBSOTf (0.529 g, 0.46 ml, 2.00 mmol) was added. The mixture was stirred at room temperature for 18.5 h. After addition of water, the resulting mixture was extracted with AcOEt. The organic layer was washed with brine, dried with Na_2SO_4,

filtrated and concentrated. The crude product was purified by silica gel column chromatography (*n*-hexane/AcOEt = 20/1 (v/v)) then recrystaized from $CHCl_3$ and MeOH to give **2** as a white solid (0.167 g, 0.341 mmol, 34 %). ^{1}H NMR (400 MHz, CD_2Cl_2): δ (ppm) 8.01 (1H, d, *J* = 8.4 Hz, Ar-*H*), 7.62 (1H, dd, *J* = 8.0, 1.2 Hz, Ar-*H*), 7.48–7.30 (4H, Ar-*H*), 7.00 (1H, dd, *J* = 7.2, 2.0 Hz, Ar-*H*), 3.09–1.36 (10H, br, B-*H*), 0.98 (9H, s, C*H*$_3$) , 0.07 (3H, s, C*H*$_3$) , –0.31 (3H, s, C*H*$_3$). ^{13}C NMR (100 MHz, CD_2Cl_2): δ (ppm) 143.4, 142.0, 134.9, 134.7, 132.7, 132.6, 130.9, 130.6, 129.9, 128.8, 127.0, 126.3, 89.6, 83.0, 31.0, 27.1, 26.8, 20.8, –3.9, –5.8. ^{11}B NMR (128 MHz, CD_2Cl_2): δ (ppm) 1.0, 0.6, –1.8, –2.9, –6.3, –7.5, –10.1, –11.4. HRMS (*n*-APCI): Calcd. for $C_{20}H_{33}B_{10}BrSi$ $[M]^-$ m/z 490.2523, found m/z 490.2516.

Synthesis of B(4)-TBS. The mixture of **2** (0.147 g, 0.30 mmol), $Pd(OAc)_2$ (0.0068 g, 0.030 mmol), P(*t*Bu)$_3$H·BF_4 (0.0172 g, 0.059 mmol), and Cs_2CO_3 (0.197 g, 0.61 mmol) were dissolved in dry toluene (12 ml) at room temperature under N_2 atmosphere. The resulting mixture was refluxed for 5 h. After hydrolysis with water and extraction with AcOEt, the combined organic phase was washed with brine and dried over Na_2SO_4. After filtration, the solvent was evaporated. The residue was purified by column chromatography on a silica gel (*n*-hexane/AcOEt = 20:1 (v/v)) to give a brown solid (0.113 g, 0.28 mmol, 92%). Further purification by recrystallization from MeOH and $CHCl_3$ can be performed for optical measurments. ^{1}H NMR (400 MHz, CD_2Cl_2): δ (ppm) 8.337.85–8.317.82 (1H, m, Ar-*H*), 8.217.73–8.197.71 (1H, m, Ar-*H*), 7.7931 (1H, dd, *J* = 8.0, 1.2 Hz, Ar-*H*), 7.7527 (1H, dd, *J* = 7.2, 0.8 Hz, Ar-*H*), 7.5709 (1H, ddd, *J* = 8.0, 7.2, 1.6 Hz, Ar-*H*) , 7.5002 (1H, ddd, *J* = 8.0, 7.2, 1.6 Hz, Ar-*H*) , 7.426.93 (1H, ddd, *J* = 7.6, 7.6, 0.8 Hz, Ar-*H*) , 7.356.87 (1H, ddd, *J* = 8.0, 7.6, 1.2 Hz, Ar-*H*), 3.6109–1.6016 (9H, br, B-*H*) , 0.8941 (9H, s, C*H*$_3$), 0.4800 (3H, s, C*H*$_3$), –0.0148 (3H, s, C*H*$_3$). ^{13}C NMR (100 MHz, CD_2Cl_2): δ (ppm) 136.6, 134.1, 133.5, 130.9, 130.4, 129.6, 129.1, 128.5, 127.0, 126.7, 124.3, 85.2, 85.0, 31.0, 27.1, 21.0, –1.8, –3.5. ^{11}B NMR (128 MHz, $CDCl_3$): δ (ppm) 1.4, 0.4, –4.8, –5.7, –6.8, –8.3, –9.8, –10.6, –12.9, –14.1. HRMS (*n*-APCI): Calcd. for $C_{20}H_{32}B_{10}Si$ $[M]^-$ m/z 410.3209, found m/z 410.3216.

Synthesis of B(3). The mixture of **1** (0.150 g, 0.40 mmol), $Pd(OAc)_2$ (0.0058 g, 0.026 mmol), P(*t*Bu)$_3$H·BF_4 (0.0117 g, 0.040 mmol), and Cs_2CO_3 (0.263 g, 0.81 mmol) were dissolved in dry MeCN (16 ml) at room temperature under N_2 atmosphere. The resulting mixture was heated at 60 °C for 4.5 h. After hydrolysis with water and extraction with $CHCl_3$, the combined organic phase was

washed with brine and dried over Na_2SO_4. After filtration, the solvent was evaporated. The residue was purified by column chromatography on a silica gel (*n*-hexane/AcOEt = 20:1 (v/v)). After evaporation of solvents, the desired product was isolated with recrystallization from $CHCl_3$ / MeOH (60 °C) as a colorless solid (0.0196 g, 0.067 mmol, 17%). ^{1}H NMR (400 MHz, $CDCl_3$): δ (ppm) 8.21 (1H, d, *J* = 7.6 Hz, Ar-*H*), 8.14 (1H, d, *J* = 8.4 Hz, Ar-*H*), 8.01 (1H, dd, *J* = 7.6, 1.2 Hz, Ar-*H*), 7.81 (1H, d, *J* = 8.0, 1.2 Hz, Ar-*H*), 7.58–7.52 (2H, m, Ar-*H*), 7.47 (1H, dd, *J* = 7.2, 7.2, 0.8 Hz, Ar-*H*), 7.37 (1H, ddd, *J* = 7.8, 7.6, 1.2 Hz, Ar-*H*), 3.16 (1H, s, carborane_C-*H*), 3.63–1.39 (9H, br, B-*H*). ^{13}C NMR (100 MHz, $CDCl_3$): δ (ppm) 135.5, 133.8, 133.7, 132.5, 130.9, 130.3, 128.6, 128.6, 128.0, 125.2, 124.0, 73.7, 60.0. ^{11}B NMR (128 MHz, $CDCl_3$): δ (ppm) –1.6, –2.7, –5.4, –6.6, –8.6, –9.8, –11.3, –12.1, –12.6. HRMS (*n*-APCI): Calcd. for $C_{14}H_{18}B_{10}$ $[M]^-$ m/z 296.2345, found m/z 296.2336.

Synthesis of B(4). The mixture of **B(4)-TBS** (0.082 g, 0.20 mmol) and CsF (0.119 g, 0.79 mmol) were dissolved in dry acetone (5 ml) at room temperature under N_2 atmosphere. The resulting mixture was stirred at room temperature for 2.5 h. After filtration, the solution was evaporated to afford yellow crude oil. The oil was purified by column chromatography on a silica gel (*n*-hexane/AcOEt = 20:1 (v/v)). After evaporation of solvents, the desired product was isolated with recrystallization from *n*-hexane (65 °C) as a colorless solid (0.0131 g, 0.044 mmol, 22%). ^{1}H NMR (400 MHz, $CDCl_3$): δ (ppm) 8.31 (1H, dd, *J* = 8.4, 0.4 Hz, Ar-*H*), 8.19 (1H, d, *J* = 8.0 Hz, Ar-*H*), 7.76 (1H, d, *J* = 7.2 Hz, Ar-*H*), 7.56–7.48 (2H, m, Ar-*H*), 7.45–7.33 (3H, m, Ar-*H*), 4.31 (1H, s, carborane_C-*H*), 3.63–1.15 (9H, br, B-*H*). ^{13}C NMR (100 MHz, $CDCl_3$): δ (ppm) 135.0, 133.6, 132.6, 130.1, 129.2, 128.9, 128.4, 127.6, 125.8, 125.7, 124.1, 73.3, 63.0. ^{11}B NMR (128 MHz, $CDCl_3$): δ (ppm) –1.1, –2.2, –6.3, –7.4, –8.8, –9.9, –10.8, –12.2, –13.7, –15.9, –17.2. HRMS (*n*-APCI): Calcd. for $C_{14}H_{18}B_{10}$ $[M]^-$ m/z 296.2345, found m/z 296.2334.

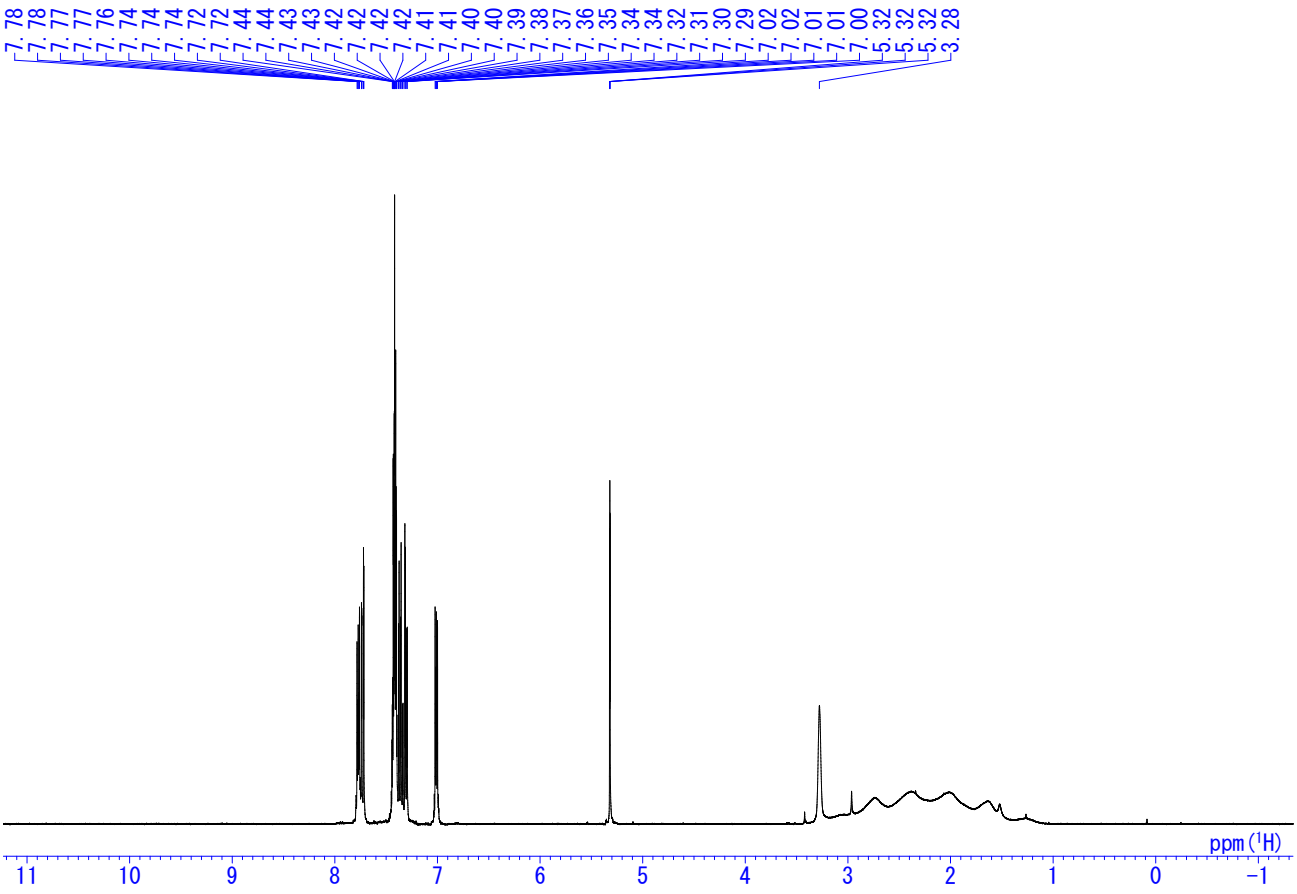

Chart S1. ^{1}H NMR spectrum of **1** in CD_2Cl_2.

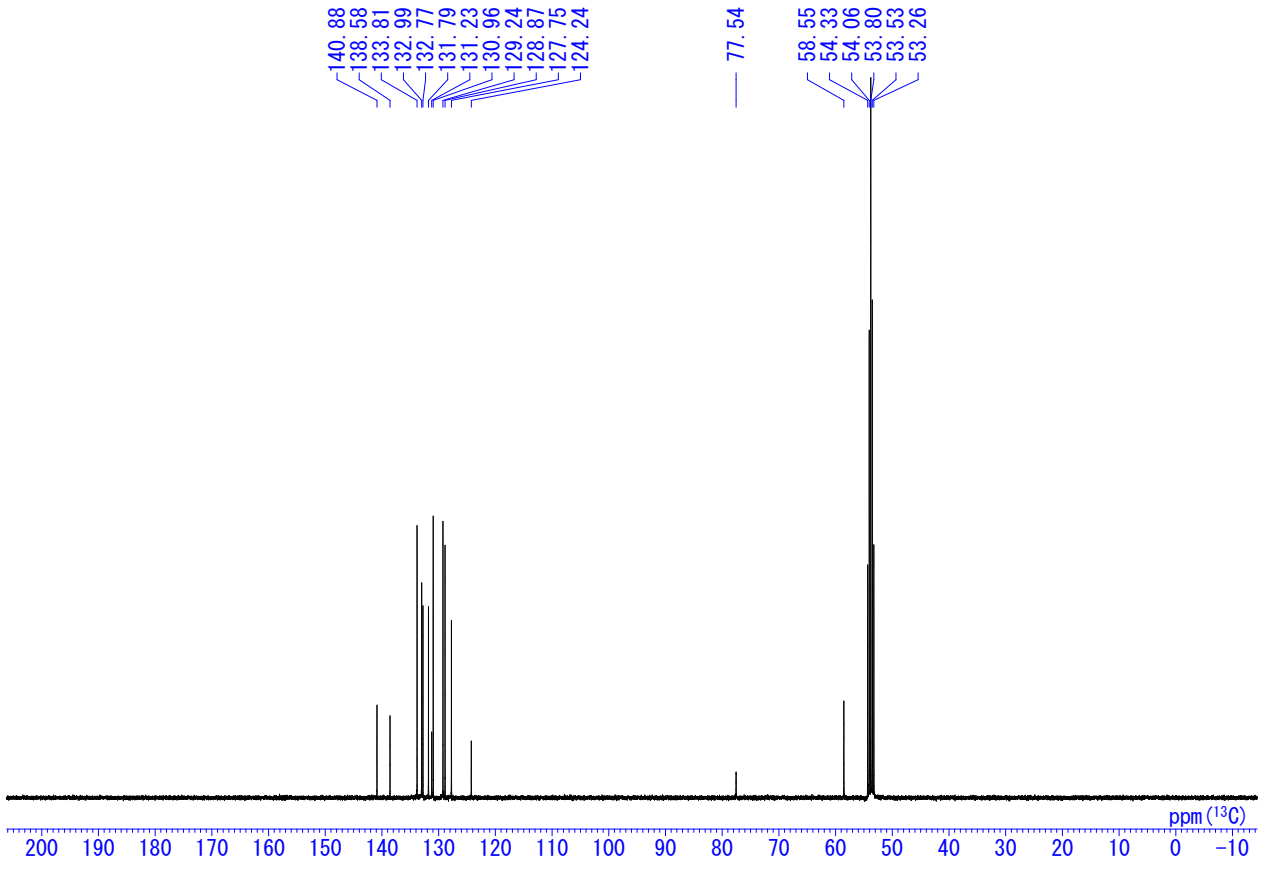

Chart S2. ^{13}C NMR spectrum of **1** in CD_2Cl_2.

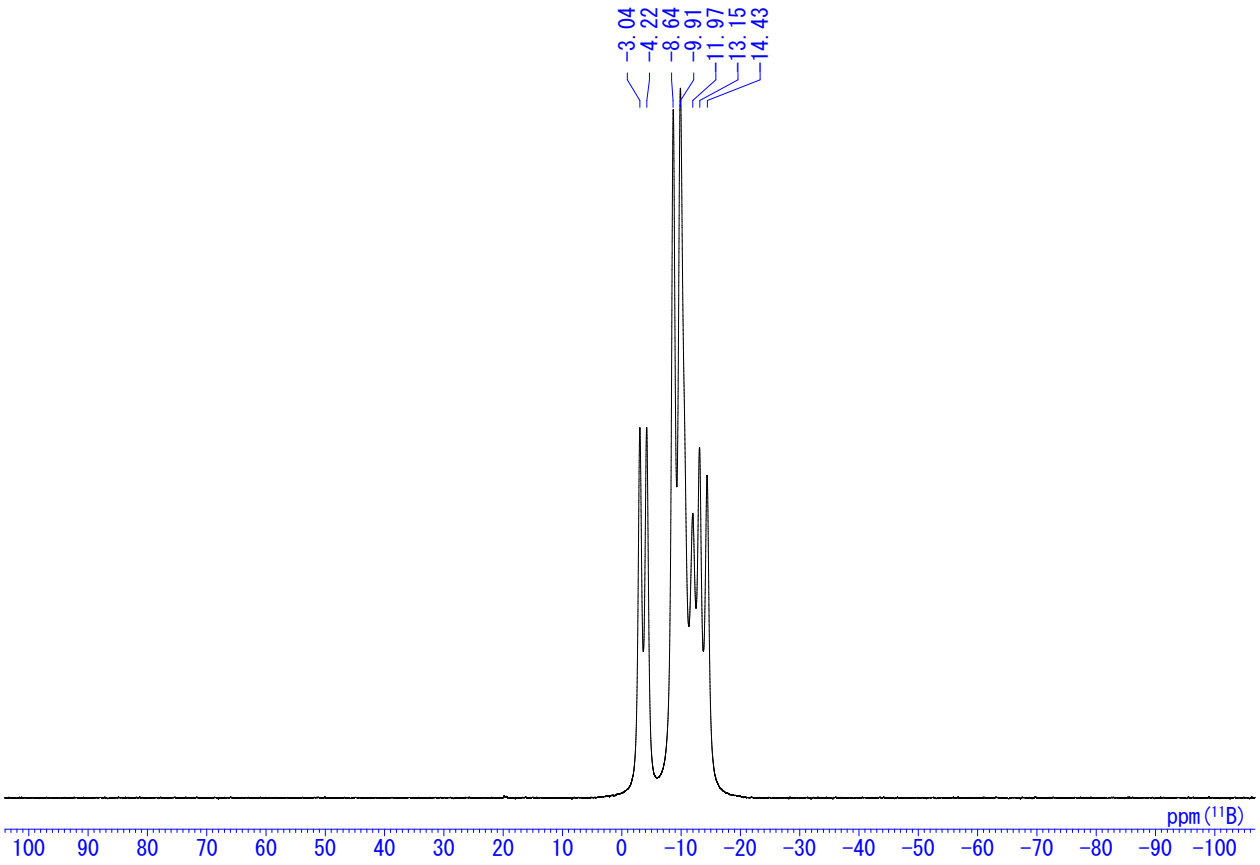

Chart S3. ^{11}B NMR spectrum of **1** in CD_2Cl_2.

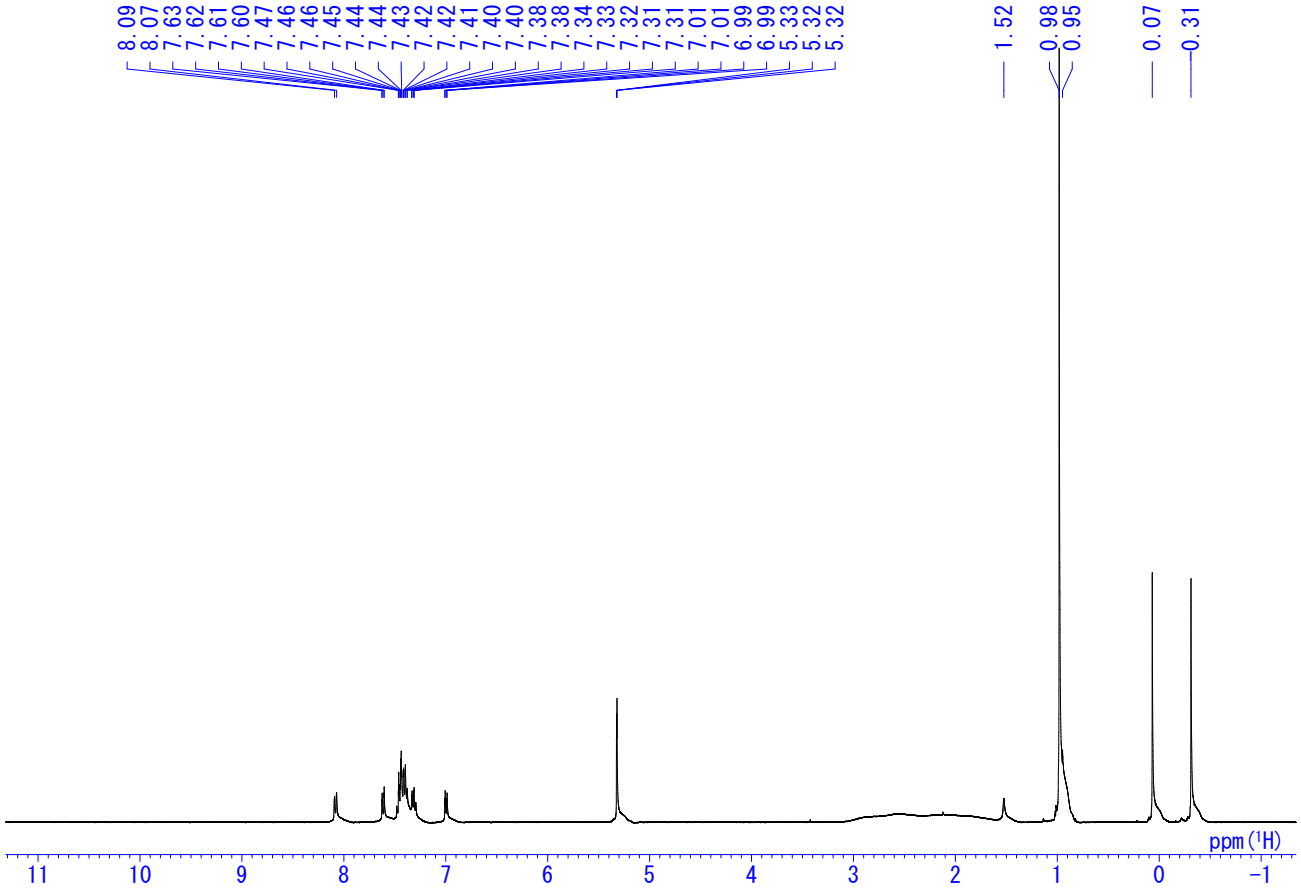

Chart S4. ^{1}H NMR spectrum of **2** in CD_2Cl_2.

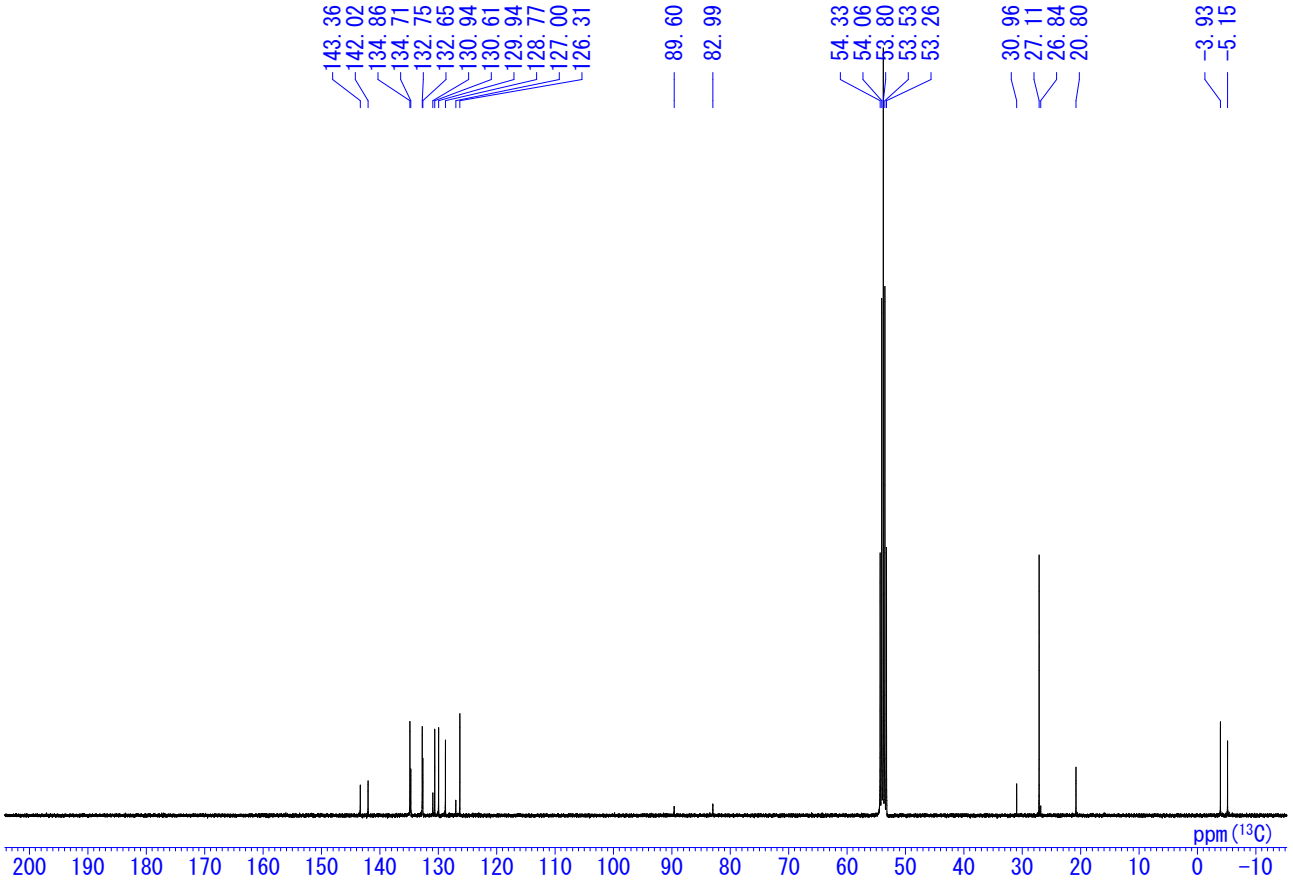

Chart S5. ^{13}C NMR spectrum of **2** in CD_2Cl_2.

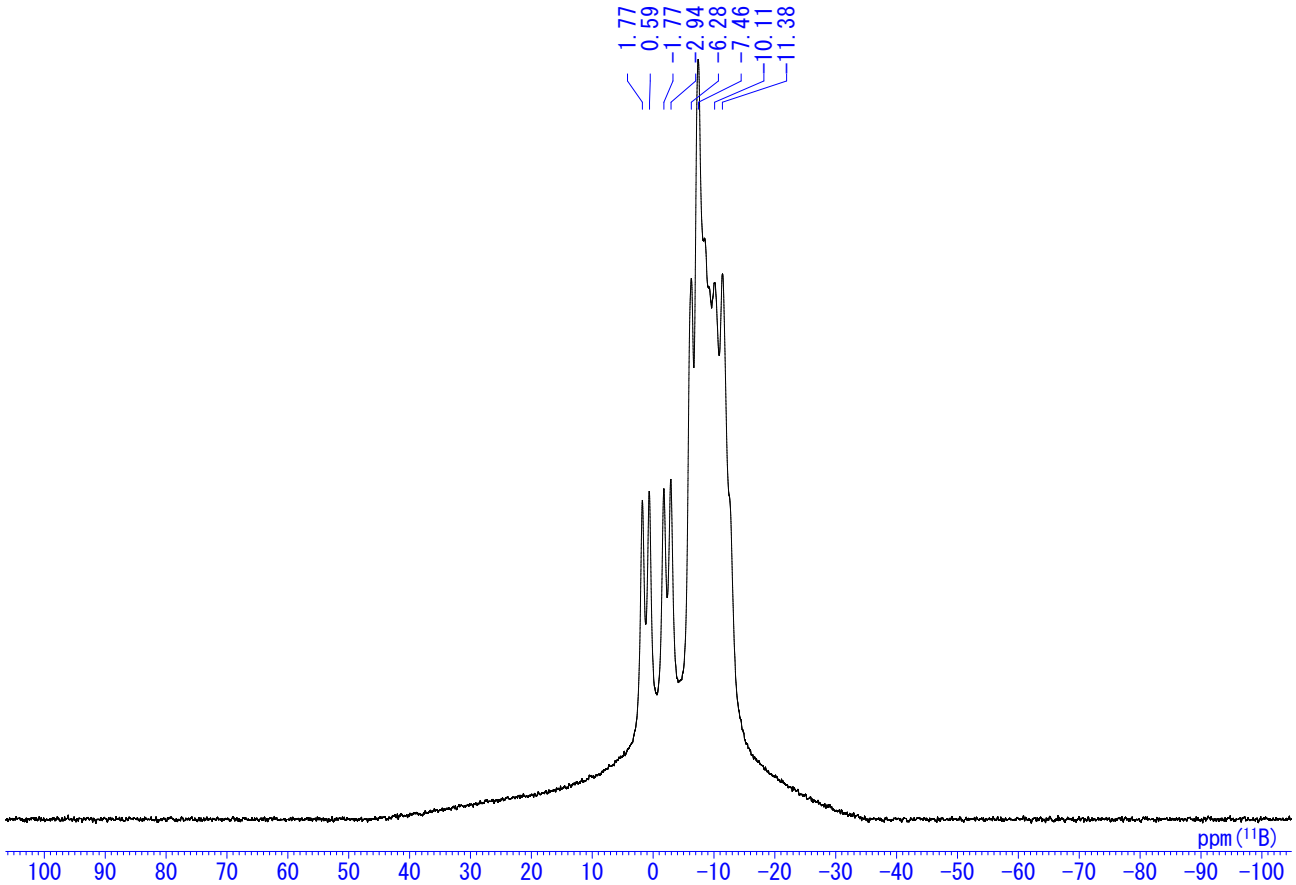

Chart S6. ^{11}B NMR spectrum of **2** in CD_2Cl_2.

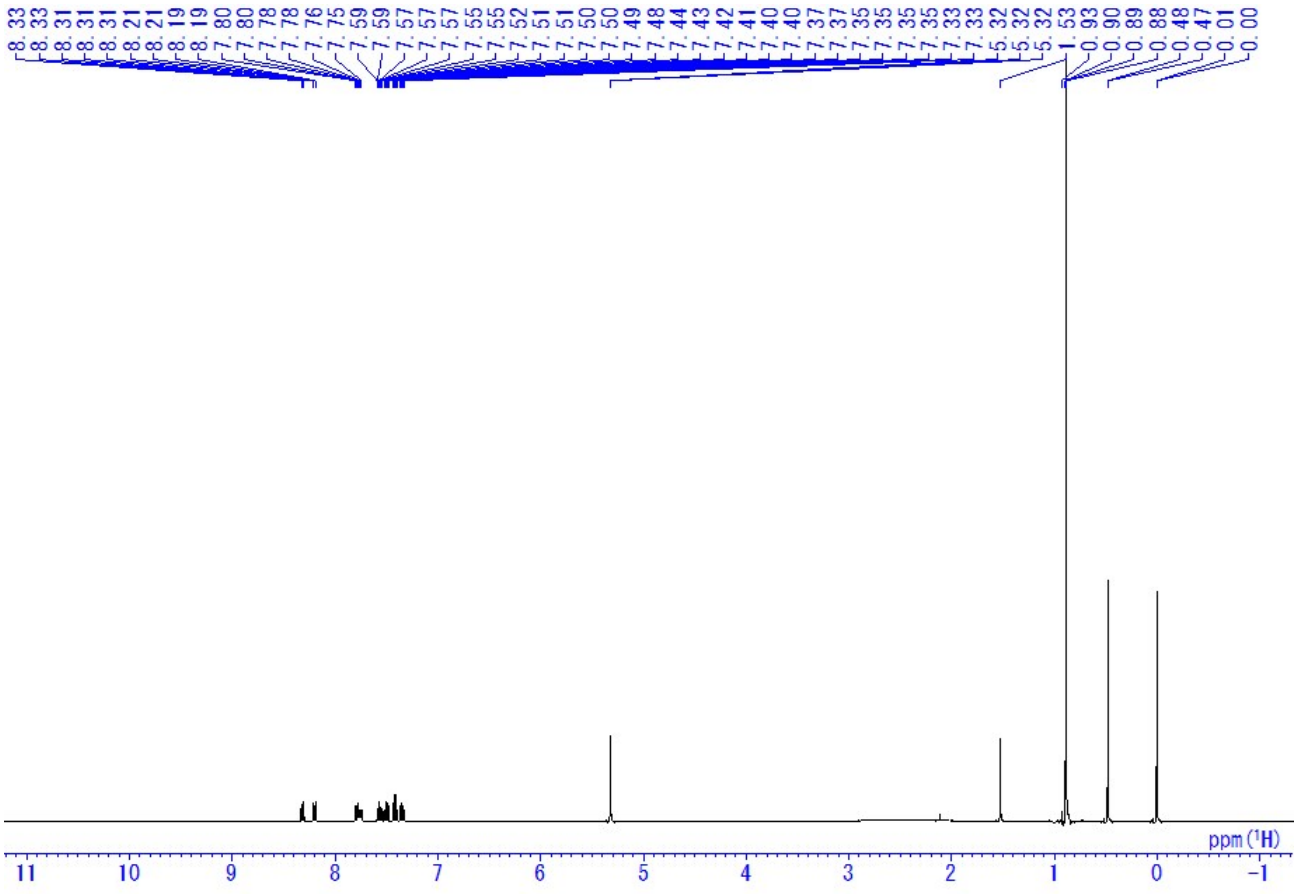

Chart S7. ^{1}H NMR spectrum of **B(4)-TBS** in CD_2Cl_2.

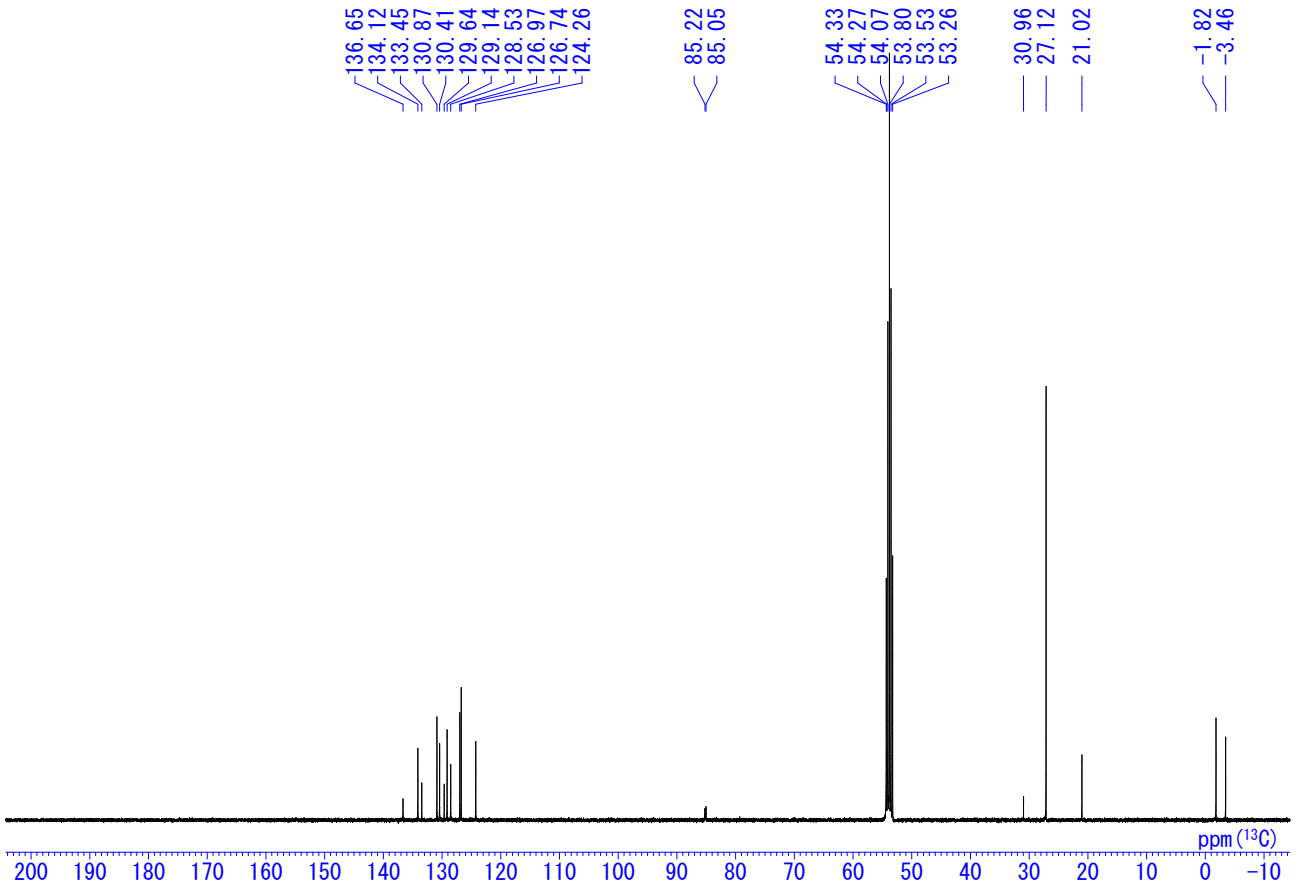

Chart S8. ^{13}C NMR spectrum of **B(4)-TBS** in CD_2Cl_2.

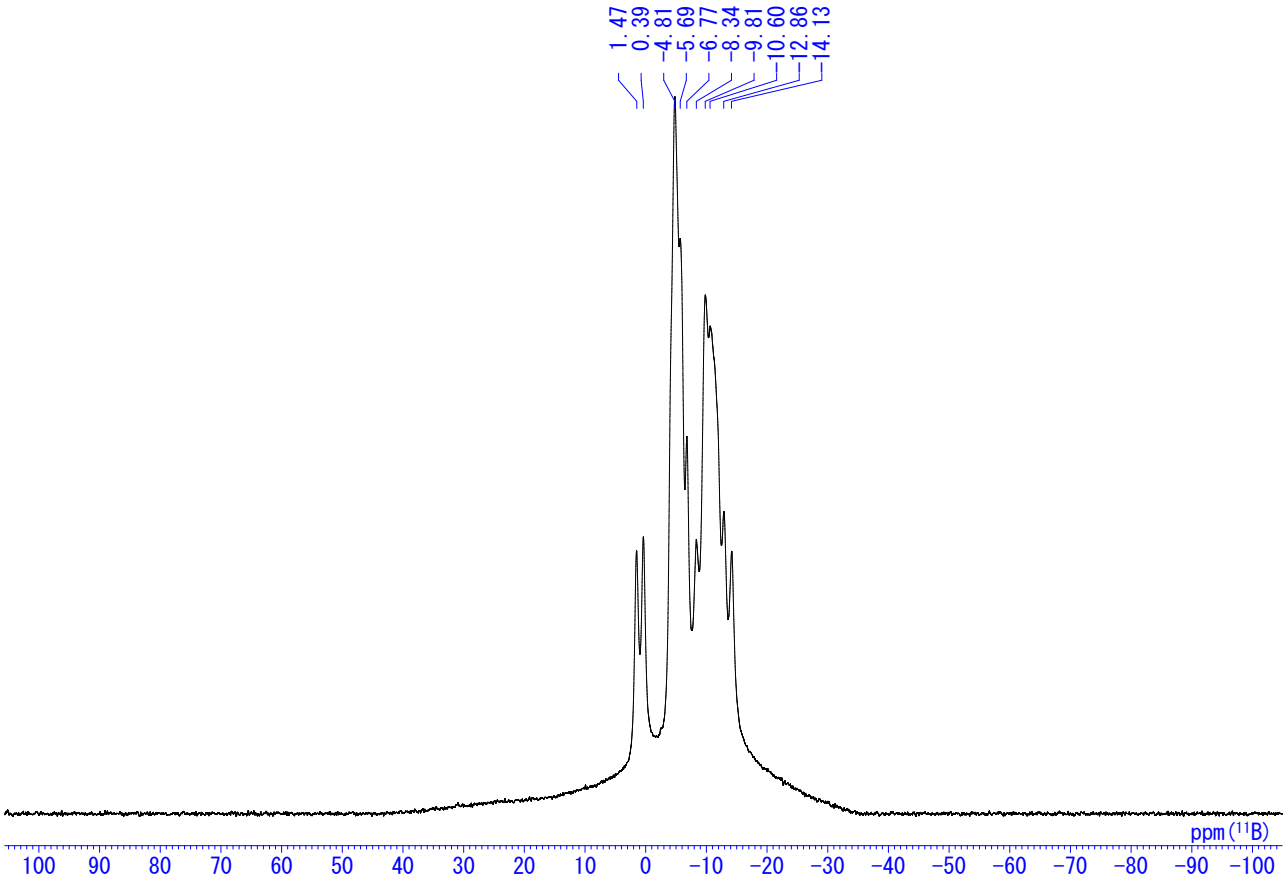

Chart S9. ^{11}B NMR spectrum of **B(4)-TBS** in CD_2Cl_2.

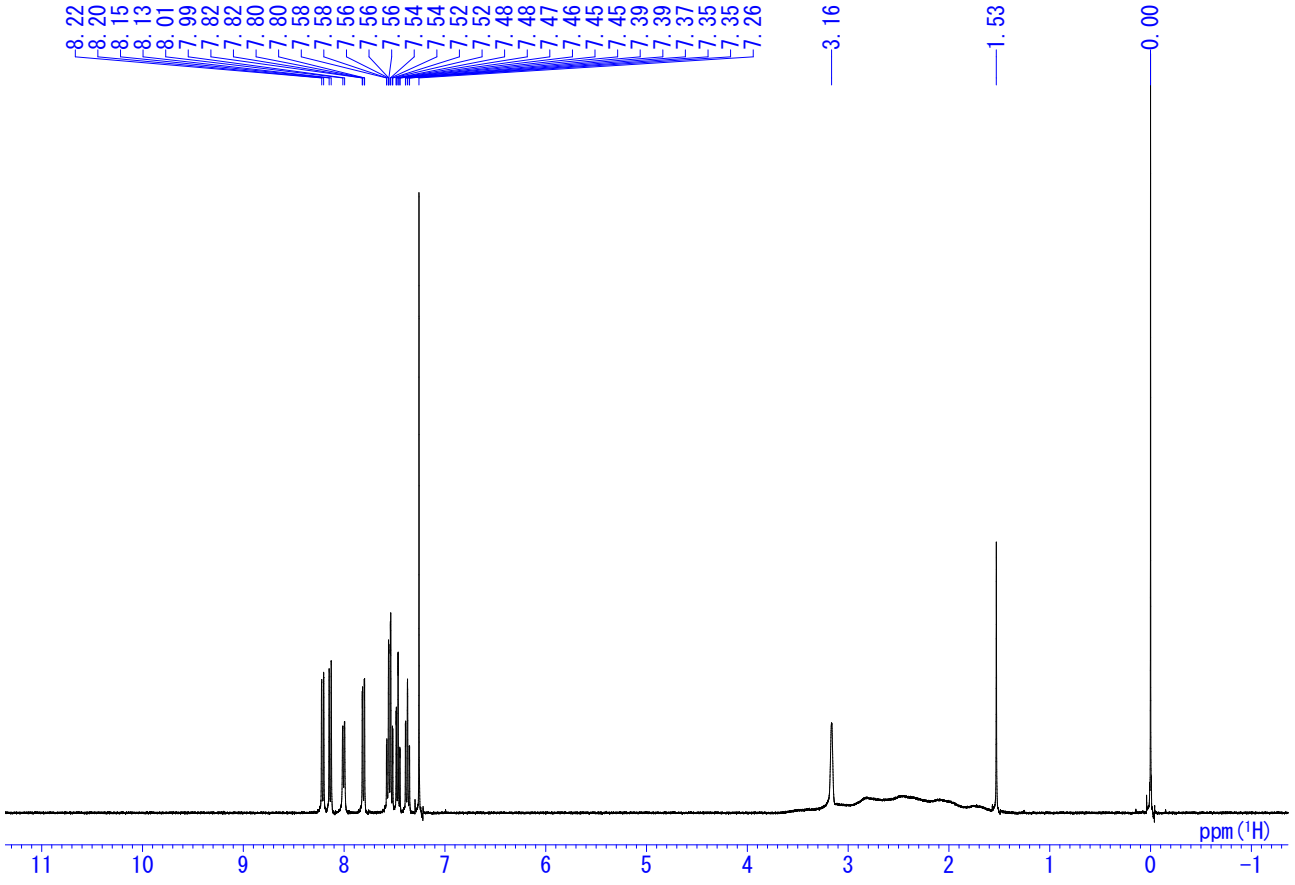

Chart S10. ^{1}H NMR spectrum of **B(3)** in $CDCl_3$.

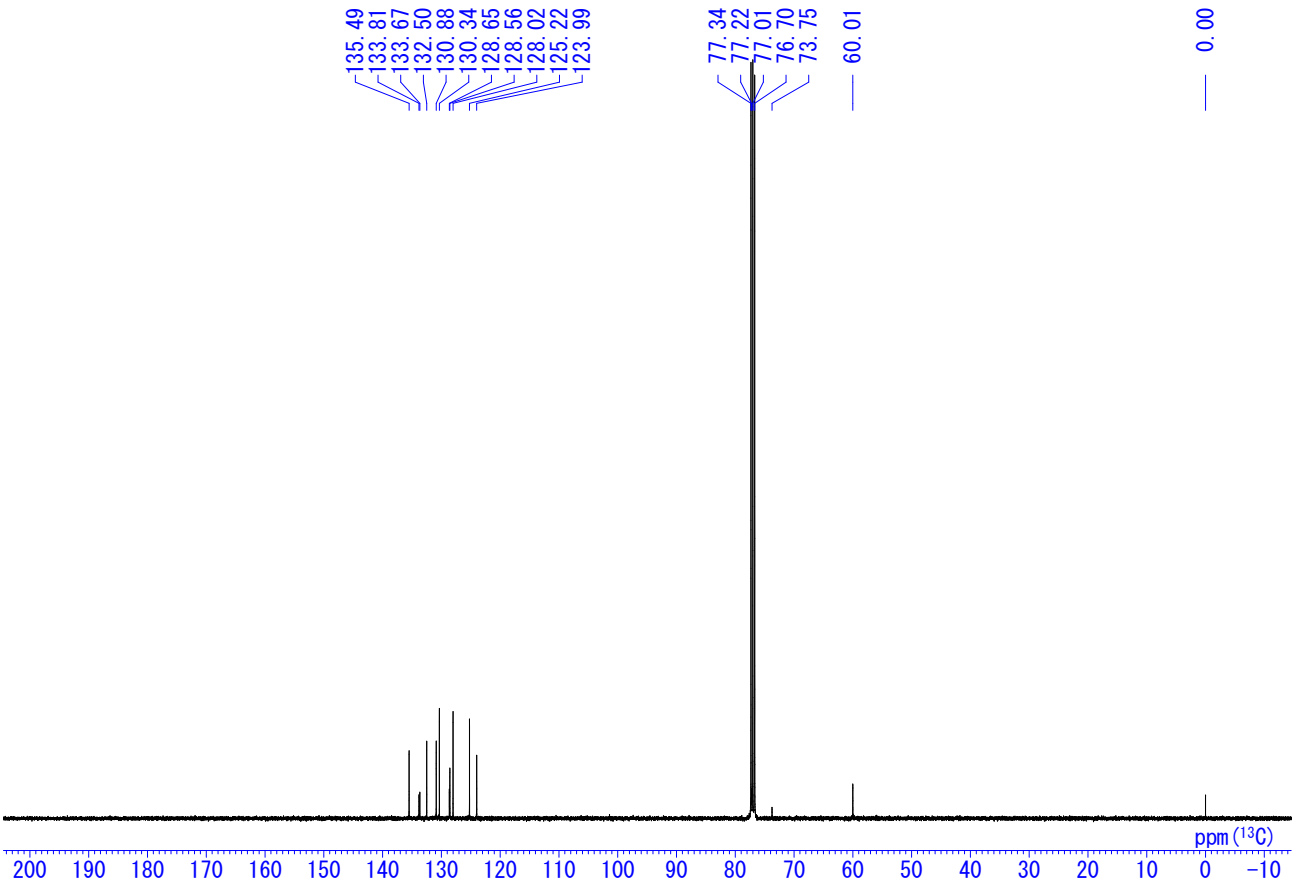

Chart S11. ^{13}C NMR spectrum of **B(3)** in $CDCl_3$.

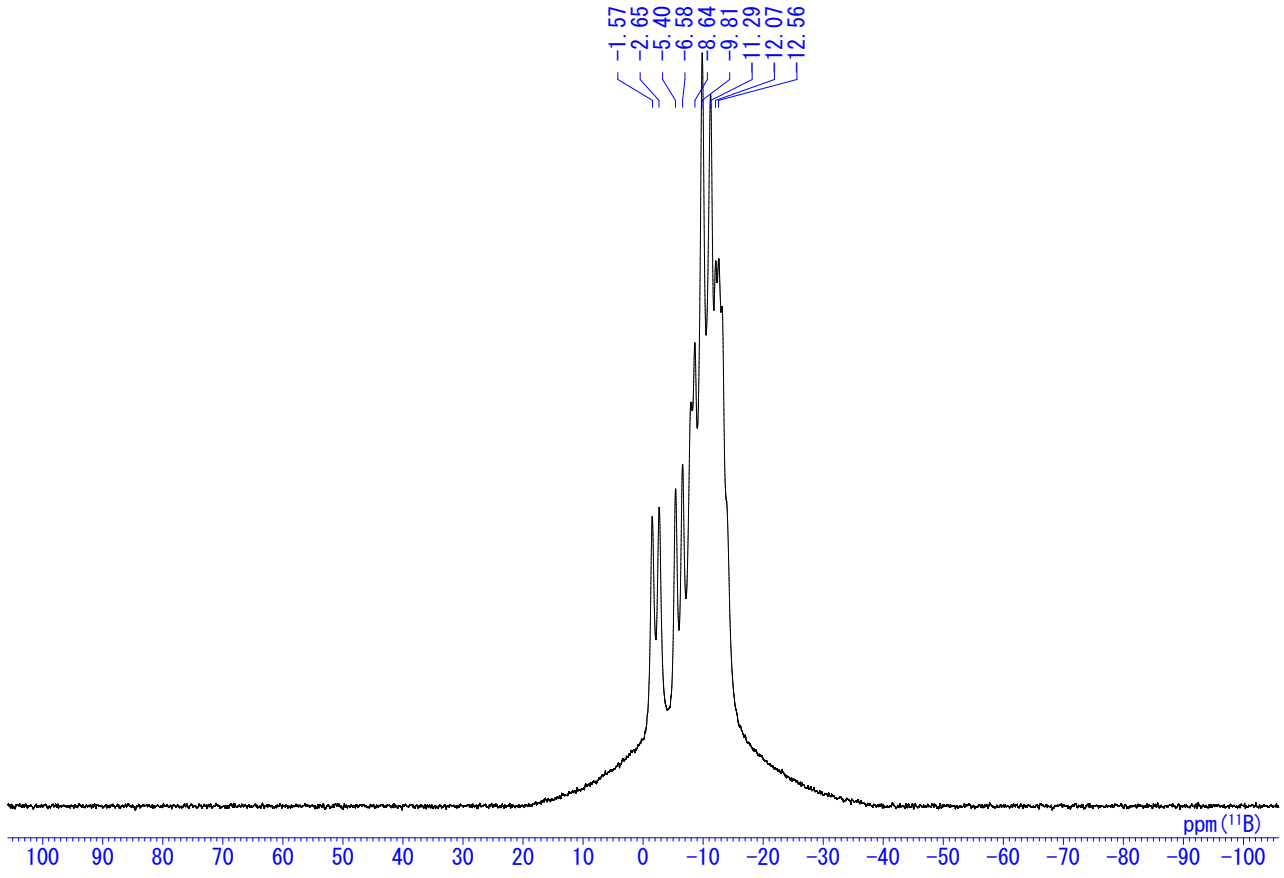

Chart S12. ^{11}B NMR spectrum of **B(3)** in $CDCl_3$.

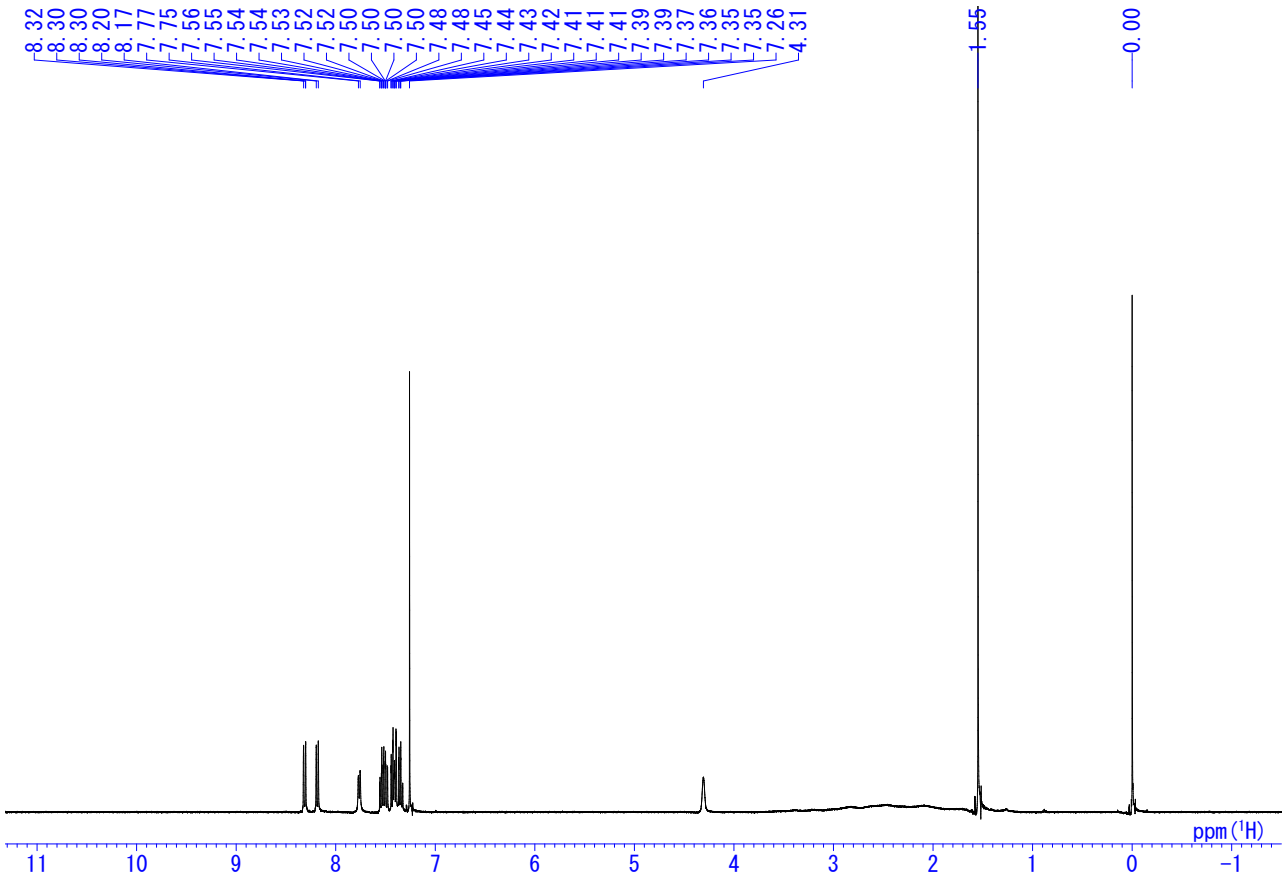

Chart S13. ^{1}H NMR spectrum of **B(4)** in $CDCl_3$.

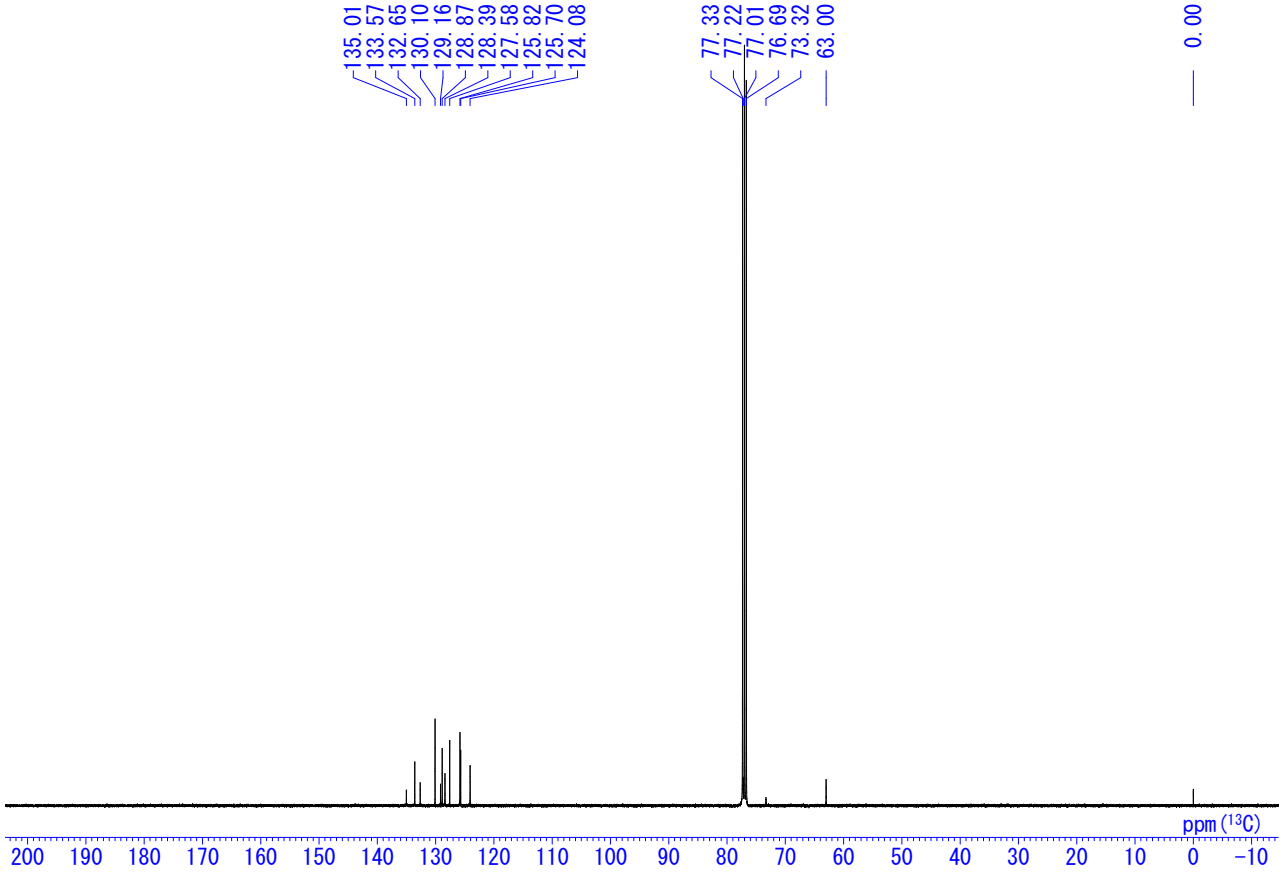

Chart S14. ^{13}C NMR spectrum of **B(4)** in $CDCl_3$.

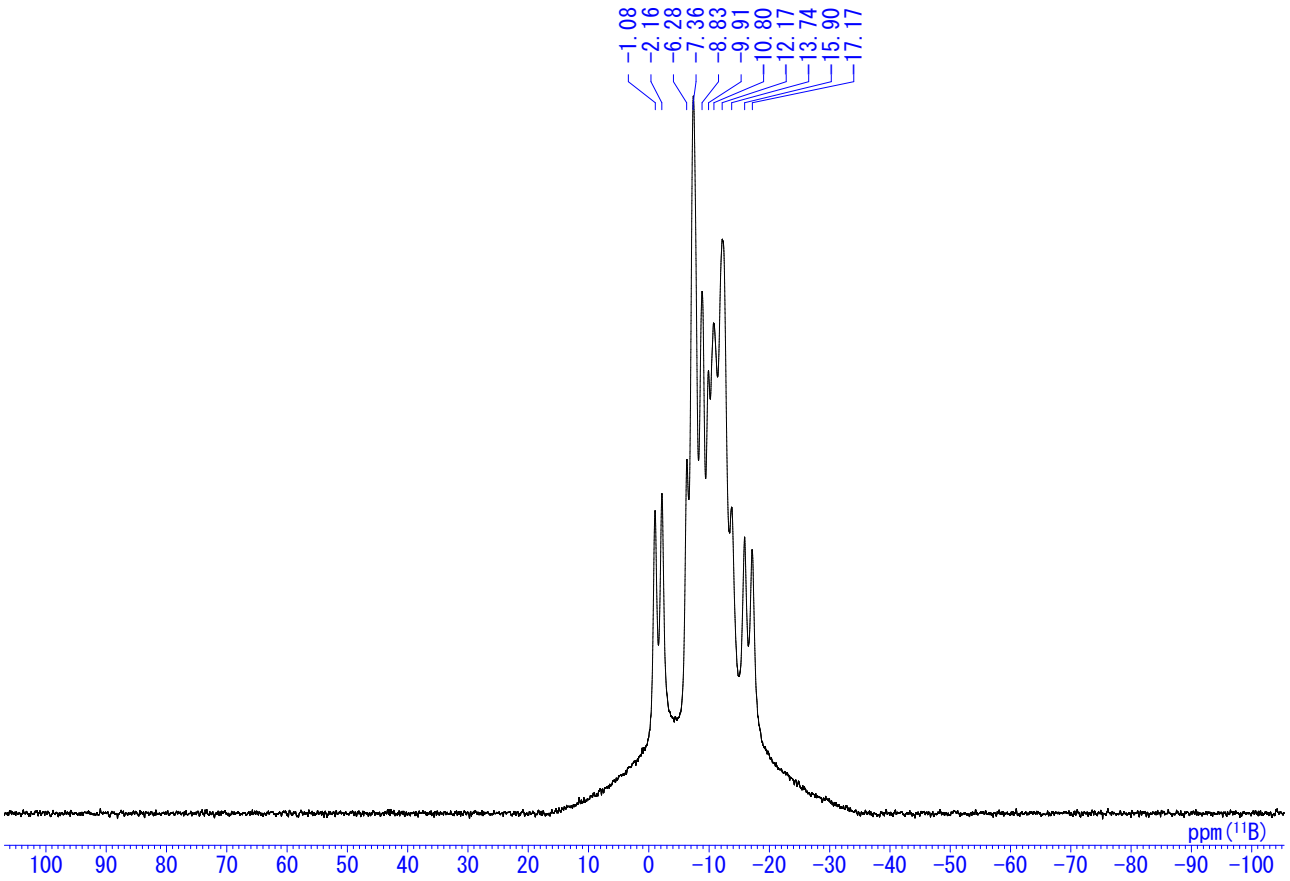

Chart S15. ^{11}B NMR spectrum of **B(4)** in $CDCl_3$.

Single Crystal X-ray Structures.

Table S1. Crystallographic data of **B(3)** (CCDC: 2032807)

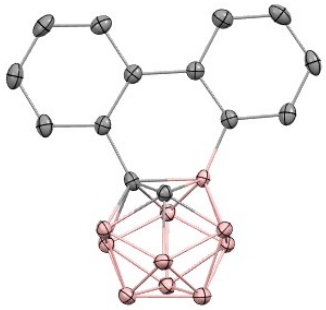

Empirical formula	$C_{14}H_{18}B_{10}$
Formula weight	294.38
Temperature (K)	93(2)
Wavelength (Å)	0.71075
Crystal system, space group	Monoclinic, $P2_1/c$
Unit cell dimensions	a = 11.0157(10)
	b = 14.0510(10)
	c = 20.5785(15)
	α = 90
	β = 72.719(7)
	γ = 90
V (Å^3)	3181.6(4)
Z, calculated density (Mg m^{-3})	8, 1.229
Absorption coefficient	0.060
F(000)	1216
Crystal size (mm)	0.50 × 0.50 × 0.30
θ range for data collection	2.351 –27.455
Limiting indices	$-14 \le h \le 14$, $-18 \le k \le 17$, $-26 \le l \le 26$
Reflections collected (unique)	29478/7247 [R(int) = 0.0580]
Goodness-of-fit on F^2	1.107
Final R indices [$I > 2\sigma(I)$]	R_1 = 0.0662, wR_2 = 0.1424
R indices (all data)	R_1 = 0.0880, wR_2 = 0.1511

Table S2. Crystallographic data of **B(4)** (CCDC: 2032808)

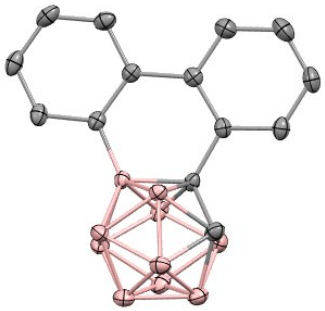

Empirical formula	$C_{14}H_{18}B_{10}$
Formula weight	294.38
Temperature (K)	83(2)
Wavelength (Å)	0.71075
Crystal system, space group	Monoclinic, $P2_1/c$
Unit cell dimensions	a = 11.1424(4)
	b = 13.9931(4)
	c = 20.6658(6)
	α = 90
	β = 92.798(7)
	γ = 90
V (Å^3)	3218.30(18)
Z, calculated density (Mg m^{-3})	8, 1.215
Absorption coefficient	0.059
F(000)	1216
Crystal size (mm)	0.75 × 0.25 × 0.10
θ range for data collection	2.338 –27.485
Limiting indices	$-14 \le h \le 14$, $-17 \le k \le 18$, $-26 \le l \le 26$
Reflections collected (unique)	50386/7376 [R(int) = 0.0544]
Goodness-of-fit on F^2	1.104
Final R indices [$I > 2\sigma(I)$]	R_1 = 0.0599, wR_2 = 0.1334
R indices (all data)	R_1 = 0.0766, wR_2 = 0.1410

Table S3. Structural information of B(3) and B(4) obtained from X-ray crystallography

		Cc_{age}–C_{cage} / Å	C_{cage}–C_{Aryl} / Å	B_{cage}–C_{Aryl} / Å	C_{cage}–C_{cage} –C_{Aryl} –C_{Aryl} / °
B(3)	Molecule 1	1.660(3)	1.511(3)	1.551(3)	65.6(2)
	Molecule 2	1.664(3)	1.511(3)	1.548(3)	63.4(2)
B(4)	Molecule 1	1.669(2)	1.503(2)	1.549(2)	42.4(2)
	Molecule 2	1.664(2)	1.499(2)	1.550(2)	40.1(2)

Optical data

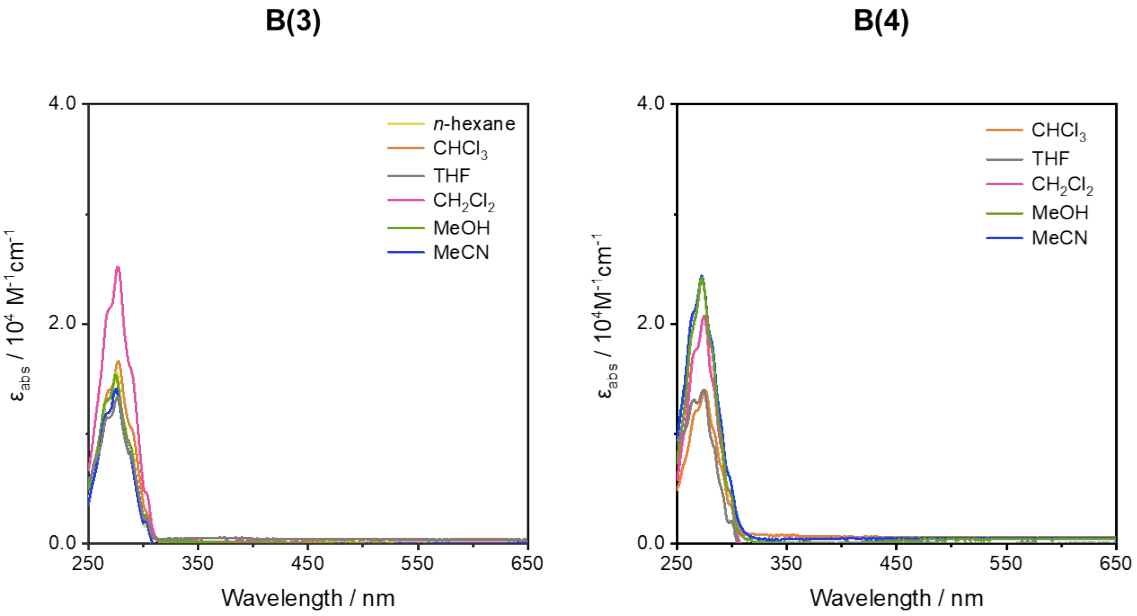

Figure S1. Absorption spectra of **B(3)** and **B(4)** in various solvents.

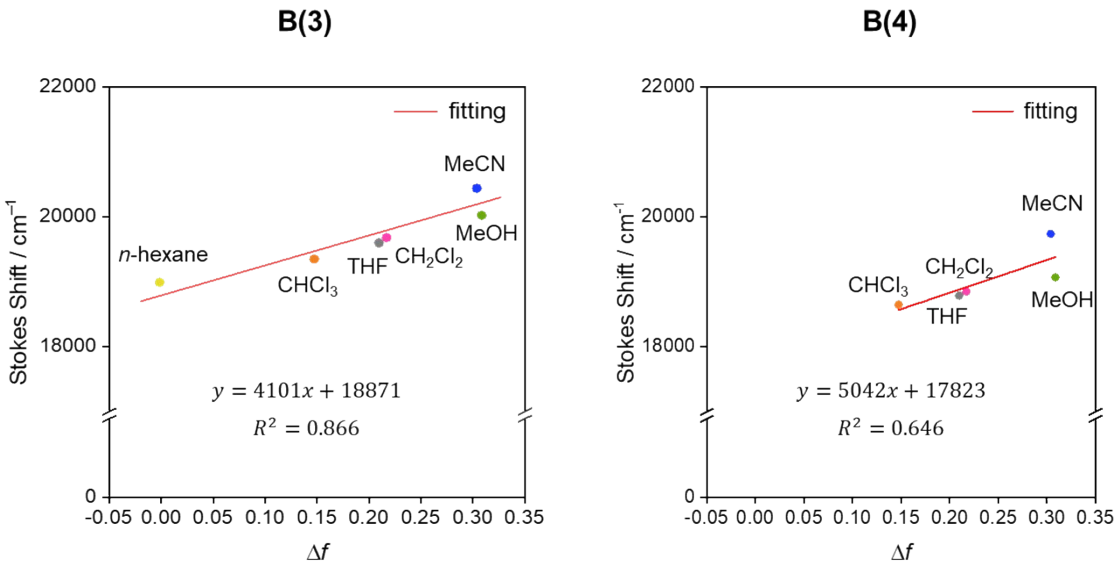

Figure S2. Lippert-Mataga plots of **B(3)** and **B(4)**.

Table S4. Absorption (Abs.) and fluorescence (FL) wavelengths of **B(3)** and **B(4)** in various solvents

		n-hexane	$CHCl_3$	THF	CH_2Cl_2	MeOH	MeCN
B(3)	Abs. / nm	276	277	277	277	275	275
	FL / nm	580	597	606	609	612	628
B(4)	Abs. / nm	---	275	275	275	273	273
	FL / nm	---	565	569	571	570	592

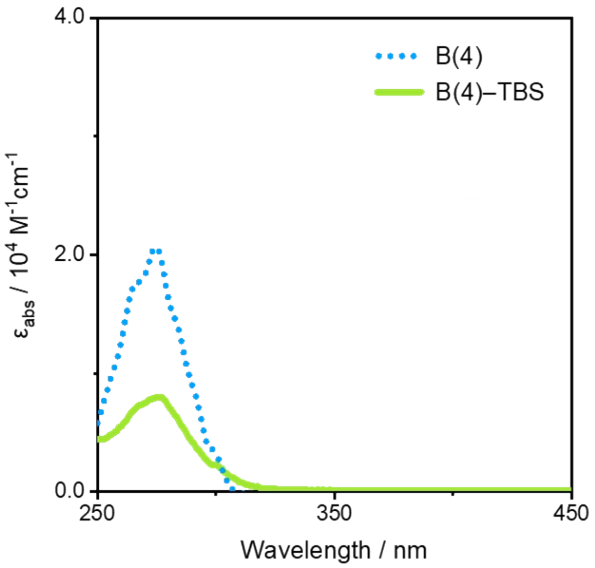

Figure S3. Absorption spectra of **B(4)** and **B(4)-TBS** in 1.0×10^{-5} M CH_2Cl_2 solutions.

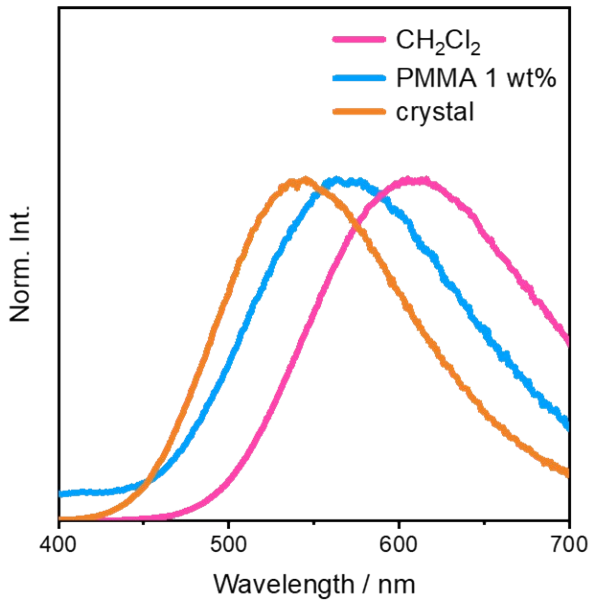

Figure S4. PL spectra of homogeneous **B(3)**-loaded film (1 wt%) with poly(methyl methacrylate) (PMMA) film.

Computational methods.

All calculations were performed using Gaussian 16 B01 package[7] at PBE1PBE-D3/6-31+G(d,p) level of theory.[8]

One isolated molecule

The potential energy curve and optimized structure were calculated by the density functional theory (DFT) for S_0 state and time dependent-DFT (TD-DFT) for S_1 state. Because S_1 structural optimization of **B(4)** from pristine S_0 optimized structure was trapped by local minimum structure, C_{cage}–C_{cage} bond of S_0 optimized structure was elongated to 2.0 Å and the structure was treated as an initial structure. We performed the frequency calculation at the optimized structure to confirm that the structure was at the local minimum because no imaginary frequencies were found. Kohn-Sham orbitals (HOMO and LUMO) were generated from the optimized structure using GaussView 6 (isovalue: 0.02).

QM/MM analyses

The molecular coordination for QM/MM analyses was extracted from single-crystal structures. The central one molecule was treated by TD-DFT method at PBE1PBE-D3/6-31+G(d,p) level of theory. The surrounding molecules were arranged to cover the central molecule completely and modeled using the universal force field (Figure S5).

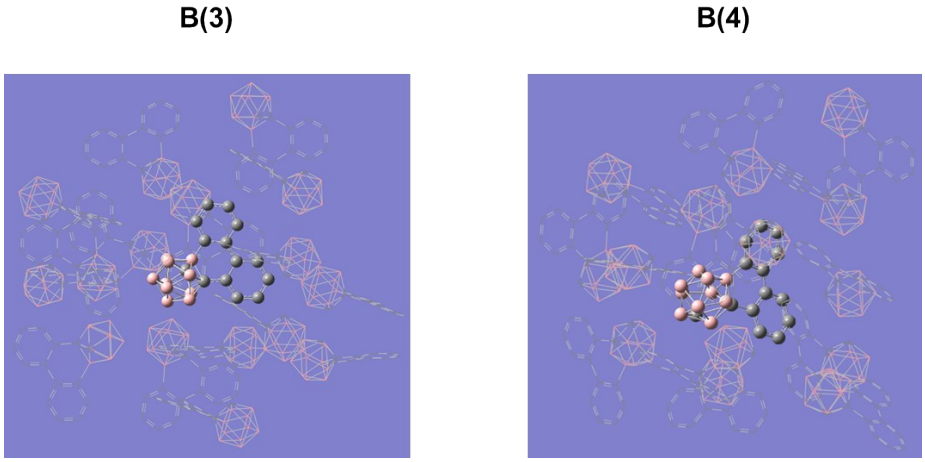

Figure S5. Setup of QM/MM model for **B(3)** (left, a cluster of 17 molecules consisting of 42 QM atoms and 672 MM atoms) and **B(4)** (right, a cluster of 17 molecules consisting of 42 QM atoms and 672 MM atoms).

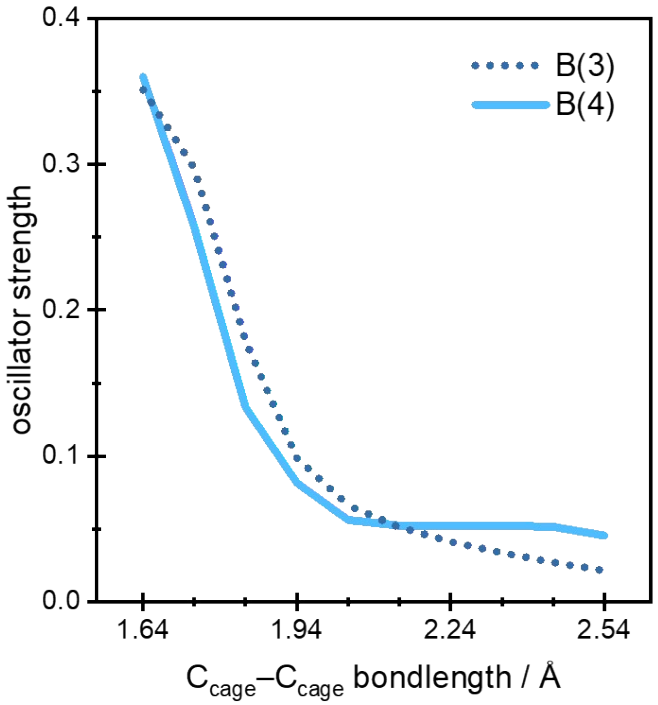

Figure S6. Influence on calculated oscillator strengths for the S_0–S_1 transition by extending C_{cage}–C_{cage} bond lengths in the S_1-optimized structures.

Table S5. Optimized geometry of **B(3)** in the S_0 state

Center Number	Atomic Number	Coordinates (Angstroms)		
		x	y	z
1	6	-0.8156	0.708677	0.074531
2	6	0.456787	1.49604	0.029872
3	6	-1.22801	-0.15807	-1.25356
4	5	-2.13506	1.233415	-0.91715
5	5	-0.61688	-0.9776	0.120519
6	5	-1.31508	-0.1043	1.494616
7	5	-2.23604	1.262562	0.853166
8	5	-2.89816	-0.25984	-1.48818
9	5	-1.95715	-1.62475	-0.85591
10	5	-3.5821	0.630503	-0.11567
11	5	-2.06418	-1.60585	0.917553
12	5	-3.07718	-0.21022	1.374792
13	5	-3.47824	-1.1587	-0.07437
14	1	-0.52821	-0.08008	-2.07843
15	6	0.847188	-1.49234	0.070764
16	1	-1.95684	2.187023	-1.59619
17	1	-2.19512	2.310935	1.407284
18	1	-0.62733	0.032218	2.451835
19	1	-1.72286	-2.56436	-1.54317
20	1	-3.29455	-0.27914	-2.60695
21	1	-4.60524	1.228546	-0.21346
22	1	-1.99295	-2.61116	1.550314
23	1	-3.74517	-0.20722	2.359222
24	1	-4.44363	-1.84951	-0.14944
25	6	1.731298	0.877579	-0.0017
26	6	1.935538	-0.59746	-0.00597
27	6	3.228201	-1.14715	-0.07746
28	6	2.843712	1.739052	-0.01583
29	6	0.345454	2.890208	0.04538
30	6	1.074986	-2.87277	0.096723
31	1	-0.64235	3.336493	0.073946
32	6	1.464156	3.70862	0.030274
33	1	3.843402	1.323874	-0.02963
34	6	2.724751	3.120148	-0.00094
35	1	3.620199	3.734723	-0.01029
36	1	1.350779	4.788096	0.043883

37	1	0.22116	-3.54199	0.163679
38	6	2.359871	-3.39546	0.037453
39	1	2.51957	-4.46951	0.058846
40	1	4.100438	-0.50912	-0.15387
41	6	3.439219	-2.51913	-0.05643
42	1	4.453715	-2.90349	-0.11308

Table S6. Optimized geometry of **B(3)** in the S_1 state

Center Number	Atomic Number	Coordinates (Angstroms)		
		x	y	z
1	6	0.585687	0.932881	-0.20209
2	6	-0.76814	1.47736	-0.06813
3	6	1.634009	-0.29628	1.572526
4	5	1.809924	1.27185	0.988657
5	5	0.809563	-0.68133	0.133752
6	5	1.138048	0.182984	-1.51471
7	5	1.897541	1.663962	-0.81217
8	5	3.190391	0.037596	1.361459
9	5	2.415144	-1.4311	0.697533
10	5	3.374921	1.174887	-0.00446
11	5	2.172562	-1.19807	-1.02712
12	5	2.897669	0.357215	-1.53203
13	5	3.662609	-0.57031	-0.241
14	1	1.175208	-0.47929	2.536776
15	6	-0.5252	-1.49584	0.12656
16	1	1.584833	2.174585	1.734147
17	1	1.772237	2.770914	-1.23374
18	1	0.408615	0.103155	-2.45269
19	1	2.484013	-2.52778	1.160352
20	1	3.890774	0.108753	2.321327
21	1	4.262493	1.967648	0.041637
22	1	2.124045	-2.16773	-1.71884
23	1	3.441237	0.516396	-2.58079
24	1	4.740015	-1.05437	-0.39871
25	6	-1.90958	0.618311	0.00718
26	6	-1.79407	-0.83161	-0.0862
27	6	-2.9414	-1.62906	-0.3265
28	6	-3.18227	1.212578	0.179189
29	6	-0.96057	2.85526	-0.03489

30	6	-0.51873	-2.89301	0.271521
31	1	-0.09231	3.500819	-0.11274
32	6	-2.2306	3.411363	0.122542
33	1	-4.05409	0.581625	0.308593
34	6	-3.34951	2.584999	0.237579
35	1	-4.33767	3.008357	0.385398
36	1	-2.33955	4.490774	0.177306
37	1	0.42804	-3.38659	0.464125
38	6	-1.66474	-3.64145	0.095544
39	1	-1.62846	-4.72469	0.16583
40	1	-3.8824	-1.16323	-0.59374
41	6	-2.88252	-2.99955	-0.23433
42	1	-3.77312	-3.59344	-0.41672

Table S7. Optimized geometry of **B(4)** in the S_0 state

Center Number	Atomic Number	Coordinates (Angstroms)		
		x	y	z
1	6	0.798094	0.648955	0.08289
2	6	-0.43005	1.495591	0.054507
3	6	2.136828	1.112154	-0.73644
4	5	1.185692	-0.11432	-1.42027
5	5	2.186955	1.157375	0.973541
6	5	1.243685	-0.24811	1.465706
7	5	0.607451	-1.01473	-0.00822
8	5	2.948347	-0.19667	-1.45151
9	5	3.561195	0.595805	0.011327
10	5	1.990524	-1.61048	-0.96532
11	5	3.011803	-0.3339	1.421934
12	5	2.030116	-1.69768	0.817685
13	5	3.477484	-1.18277	-0.07752
14	1	2.07478	2.073252	-1.23363
15	1	2.144358	2.213394	1.507049
16	1	0.492647	0.161859	-2.33971
17	6	-0.87313	-1.49722	-0.0181
18	1	0.534089	-0.15182	2.411609
19	1	4.512648	1.30249	-0.05382
20	1	3.481273	-0.01139	-2.49589
21	1	1.884607	-2.56866	-1.66252
22	1	3.647031	-0.37371	2.426339

23	1	1.953917	-2.73557	1.395619
24	1	4.469164	-1.83587	-0.14631
25	6	-1.13678	-2.87139	-0.03178
26	6	-1.94322	-0.57516	0.010512
27	6	-0.28969	2.886335	0.063803
28	6	-1.71337	0.896643	0.004077
29	6	-3.25103	-1.09307	0.048512
30	6	-2.80624	1.781228	-0.06098
31	6	-2.66074	3.159868	-0.06256
32	1	0.702454	3.321626	0.131327
33	6	-1.39115	3.726208	0.00562
34	1	-3.54277	3.791164	-0.117
35	1	-1.25861	4.803558	0.014035
36	6	-3.49623	-2.45896	0.039376
37	1	-0.2983	-3.56284	-0.05623
38	6	-2.43522	-3.36161	-0.00715
39	1	-2.62024	-4.43192	-0.01609
40	1	-4.52106	-2.81786	0.071678
41	1	-4.10896	-0.43306	0.097262
42	1	-3.8118	1.385232	-0.12419

Table S8. Optimized geometry of **B(4)** in the S_1 state

Center Number	Atomic Number	Coordinates (Angstroms)		
		x	y	z
1	6	0.65867	0.70931	0.146116
2	6	-0.59332	1.470083	0.090947
3	6	2.699797	1.165887	-0.9918
4	5	1.366718	0.152765	-1.29438
5	5	2.192542	1.335955	0.612052
6	5	1.234705	-0.00782	1.492735
7	5	0.632361	-0.88705	0.054426
8	5	3.176368	-0.31444	-1.39821
9	5	3.789866	0.564066	0.041851
10	5	2.013306	-1.53137	-0.8107
11	5	2.987551	-0.10307	1.462364
12	5	2.000657	-1.52868	0.980587
13	5	3.495576	-1.19631	0.118433
14	1	2.852482	2.038559	-1.61495
15	1	2.21194	2.422526	1.105978

16	1	0.735513	0.300615	-2.29546
17	6	-0.8289	-1.47573	-0.01811
18	1	0.621606	0.181839	2.496987
19	1	4.836576	1.123722	0.135863
20	1	3.720491	-0.46656	-2.44633
21	1	1.84776	-2.51625	-1.46491
22	1	3.556009	-0.05188	2.50795
23	1	1.863231	-2.51571	1.638763
24	1	4.416682	-1.95136	0.175273
25	6	-1.00224	-2.84939	-0.02269
26	6	-1.98516	-0.63779	-0.00737
27	6	-0.54859	2.854387	-0.01897
28	6	-1.87435	0.810815	0.072936
29	6	-3.27297	-1.25709	-0.07413
30	6	-3.03692	1.630536	0.050207
31	6	-2.96528	3.006053	-0.01491
32	1	0.422048	3.33719	-0.04056
33	6	-1.7115	3.625052	-0.05931
34	1	-3.87391	3.599166	-0.02432
35	1	-1.63755	4.707814	-0.10306
36	6	-3.41709	-2.62845	-0.09921
37	1	-0.12035	-3.48316	-0.01025
38	6	-2.27708	-3.43715	-0.07228
39	1	-2.37326	-4.51857	-0.11166
40	1	-4.40671	-3.07151	-0.14411
41	1	-4.17212	-0.6545	-0.09311
42	1	-4.01909	1.178707	0.103559

Table S9. Result of TD-DFT calculation for **B(3)** in the S_0 geometry

Excited State	**Energy / eV**	**Wavelength / nm**	***f***	**Composition**	**Coefficient**
1	4.5182	274.41	0.2917		
				HOMO -> LUMO	0.68279
2	4.6444	266.96	0.0042		
				HOMO–2 -> LUMO	0.19512
				HOMO–1 -> LUMO	–0.43441
				HOMO -> LUMO+1	0.45930
				HOMO -> LUMO+2	0.22260
3	4.7854	259.09	0.0164		0.35738
				HOMO–2 -> LUMO	0.33963
				HOMO–1 -> LUMO	–0.10840
				HOMO -> LUMO	0.33611

				HOMO -> LUMO+1	–0.33973
				HOMO -> LUMO+2	

Table S10. Result of TD-DFT calculation for **B(3)** in the S_1 geometry

Excited State	Energy / eV	Wavelength / nm	*f*	Composition	Coefficient
1	1.9678	630.05	0.0295		
				HOMO–1 -> LUMO	0.11383
				HOMO -> LUMO	–0.69357
2	2.7092	457.64	0.0098		
				HOMO–3 -> LUMO	0.12311
				HOMO–1 -> LUMO	–0.67956
				HOMO -> LUMO	–0.12476
3	3.2482	381.70	0.0860		
				HOMO–3 -> LUMO	–0.18225
				HOMO–2 -> LUMO	0.65584
				HOMO–1 -> LUMO	–0.10337

Table S11. Result of TD-DFT calculation for **B(3)** in the S_1 geometry in the QM/MM condition

Excited State	Energy / eV	Wavelength / nm	*f*	Composition	Coefficient
1	2.4188	512.59	0.0493		
				HOMO -> LUMO	0.69879
2	3.2024	387.17	0.0073		
				HOMO–3 -> LUMO	0.10903
				HOMO–1 -> LUMO	0.68623
3	3.6025	344.16	0.00845		
				HOMO–5 -> LUMO	0.10261
				HOMO–3 -> LUMO	–0.12386
				HOMO–2 -> LUMO	–0.66204
				HOMO -> LUMO+2	–0.13845

Table S12. Result of TD-DFT calculation for **B(4)** in the S_0 geometry

Excited State	Energy / eV	Wavelength / nm	*f*	Composition	Coefficient
1	4.5195	274.33	0.2540		
				HOMO–1 -> LUMO	0.19755
				HOMO–1 -> LUMO+2	–0.10358
				HOMO -> LUMO	0.65127
				GOMO -> LUMO+2	0.11117
2	4.6065	269.15	0.0209		
				HOMO–2 -> LUMO	–0.28532
				HOMO–1 -> LUMO	–0.17566
				HOMO -> LUMO+1	0.59747
				HOMO -> LUMO+2	–0.12981

3	4.7006	263.76	0.0574		
				HOMO–2 -> LUMO	–0.11785
				HOMO–1 -> LUMO	0.53148
				HOMO -> LUMO	–0.22213
				HOMO -> LUMO+1	0.19151
				HOMO -> LUMO+2	0.31722

Table S13. Result of TD-DFT calculation for **B(4)** in the S_1 geometry

Excited State	**Energy / eV**	**Wavelength / nm**	***f***	**Composition**	**Coefficient**
1	2.2715	545.82	0.0523		
				HOMO -> LUMO	0.70023
2	2.9984	413.50	0.0159		
				HOMO–4 -> LUMO	0.15886
				HOMO–2 -> LUMO	–0.48487
				HOMO–1 -> LUMO	–0.46880
3	3.1861	389.14	0.0175		
				HOMO–2 -> LUMO	0.48448
				HOMO–1 -> LUMO	0.50131

Table S14. Result of TD-DFT calculation for **B(4)** in the S_1 geometry in the QM/MM condition

Excited State	**Energy / eV**	**Wavelength / nm**	***f***	**Composition**	**Coefficient**
1	2.4716	501.63	0.0550		
				HOMO -> LUMO	0.70182
2	3.2606	380.24	0.0251		
				HOMO–4 -> LUMO	–0.14048
				HOMO–2 -> LUMO	–0.49611
				HOMO–1 -> LUMO	–0.46367
3	3.3464	370.50	0.0135		
				HOMO–2 -> LUMO	0.46412
				HOMO–1 -> LUMO	0.51823

References.

(1) Higashi, T. *ABSCOR. Program for Absorption Correction*, Rigaku Corporation, **1995**.

(2) Sheldrick, G. M. *Acta Crystallogr. Sect. A Found. Adv.*, 2014, **A71**, 3–8.

(3) Sheldrick, G. M. *Acta Crystallogr. Sect. C Struct. Chem.*, 2014, **C71**, 3–8.

(4) K. Wakita, *Yadokari-XG. Program for Crystal Structure Analysis*, 2000.

(5) C. F. Macrae, P. R. Edgington, P. McCabe, E. Pidcock, G. P. Shields, R. Taylor, M. Towler, J. van de Streek, *J. Appl. Cryst.* 2006, **39**, 453–457.

(6) A. Urbano, A. M. Hoyo, A. Martínez-Carrión, M. C. Carreño, *Org. Lett.* 2019, **21 (12)**, 4623–4627.

(7) Gaussian 16, Revision B.01, M. J. Frisch, G. W. Trucks, H. B. Schlegel, G. E. Scuseria, M. A. Robb, J. R. Cheeseman, G. Scalmani, V. Barone, G. A. Petersson, H. Nakatsuji, X. Li, M. Caricato, A. V. Marenich, J. Bloino, B. G. Janesko, R. Gomperts, B. Mennucci, H. P. Hratchian, J. V. Ortiz, A. F. Izmaylov, J. L. Sonnenberg, D. Williams-Young, F. Ding, F. Lipparini, F. Egidi, J. Goings, B. Peng, A. Petrone, T. Henderson, D. Ranasinghe, V. G. Zakrzewski, J. Gao, N. Rega, G. Zheng, W. Liang, M. Hada, M. Ehara, K. Toyota, R. Fukuda, J. Hasegawa, M. Ishida, T. Nakajima, Y. Honda, O. Kitao, H. Nakai, T. Vreven, K. Throssell, J. A. Montgomery, Jr., J. E. Peralta, F. Ogliaro, M. J. Bearpark, J. J. Heyd, E. N. Brothers, K. N. Kudin, V. N. Staroverov, T. A. Keith, R. Kobayashi, J. Normand, K. Raghavachari, A. P. Rendell, J. C. Burant, S. S. Iyengar, J. Tomasi, M. Cossi, J. M. Millam, M. Klene, C. Adamo, R. Cammi, J. W. Ochterski, R. L. Martin, K. Morokuma, O. Farkas, J. B. Foresman, and D. J. Fox, Gaussian, Inc., Wallingford CT, 2016.

(8) Q. Wu, T. Zhang, Q. Peng, D. Wang and Z. Shuai, *Phys. Chem. Chem. Phys.*, 2014, **16**, 5545–5552.